

Impact of climate change on variations in groundwater storage in the Saïss aquifer (Northern Morocco)

Chaymae Tsouli^{1,2*}, Anass Aynaou^{1,2}, Nordine Nouayti^{1,2}, Driss Khattach³ and Abderahim Nouayti⁴

¹ Laboratory of Spectroscopy, Molecular Modeling, Materials, Nanomaterials, Water and Environment (LS3MN2E), Faculty of Sciences, Rabat, Morocco.

² Environmental Management and Civil Engineering Team, Engineering Sciences and Applications Laboratory (LSIA), National School of Applied Sciences, Abdelmalek Essaadi University, Al Hoceima, Morocco.

³ Laboratory of Applied Sciences, Mohammed 1st University, Oujda, Morocco.

⁴ Laboratory of Geophysics and Natural Hazards, Scientific Institute, Rabat, Morocco.

Abstract. This study examines the influence of rainfall intensity and drought regimes on groundwater levels in the Sais aquifer, located in a semi-arid region of Morocco. Using satellite-derived datasets and the Innovative Trend Analysis (ITA) method, the research analyses groundwater storage (GWS) trends, providing a robust approach to detect long-term changes compared to the Mann-Kendall test. The study employs Gravity Recovery and Climate Experiment (GRACE) gridded data to estimate groundwater fluctuations and assess time series trends in equivalent water thickness (EWT) and soil moisture. Results indicate a significant decline in groundwater levels, with 40% of monitoring sites showing a substantial downward trend and 60% experiencing pronounced declines. The estimated maximum groundwater storage loss is $-0.244 \text{ cm/yr}^{-1}$. These findings highlight the adverse effects of overexploitation and inefficient irrigation. While the study's reliance on satellite data provides valuable information, it may overlook localized variations, and GRACE data may be less accurate in areas with complex geological features. Despite these limitations, the research informs water management strategies to mitigate groundwater depletion. The novelty of this study lies in the use of the ITA technique to enhance trend detection accuracy and support sustainable groundwater management in vulnerable regions such as the Sais aquifer.

Keywords: Groundwater levels, rainfall intensity, drought regimes, Sais aquifer, Innovative Trend Test (ITA), water management.

1 Introduction

Climate projections predict a substantial increase in temperatures, accompanied by a decrease in annual precipitation and a likely escalation of extreme rainfall events in several regions of the Mediterranean basin.[1]. As a result, vulnerability to these catastrophic food shortages and droughts could increase, particularly in developing countries.[2]

In this context, water resource management, particularly groundwater, is crucial in arid and semi-arid regions in Morocco, where water scarcity is exacerbated by climate variability and human activities [3]. The Sais aquifer is a crucial water source in the Fez Meknes region, but groundwater levels have been affected by both climate change and overexploitation.[4].

Recent advances in satellite climate data, such as those from the Gravity Recovery and Climate Experiment (GRACE), have proven effective in studying groundwater fluctuations and water storage dynamics.[5]. Although many studies have successfully applied satellite data to hydrological assessments, the integration of these data for specific aquifers, such as the Sais aquifer, remains underexplored. This study aims to fill this gap by assessing the contribution of satellite data

through understanding groundwater changes in the Sais aquifer, alongside traditional in situ measurement [6]; [7].

The main objective of this paper is to assess the impacts of precipitation and drought on groundwater fluctuations. In addition, the study will focus on identifying new patterns and trends in groundwater storage using advanced methods such as Innovative Trend Analysis (ITA) [8]. Furthermore, by exploring these relationships, the study will provide valuable information for water resources management, filling a critical gap in the scientific understanding of groundwater dynamics in semi-arid regions [9]; [10].

In summary, this study aims to improve our knowledge of the role of satellite climate data in hydrogeological studies, refine analysis techniques, and provide new insights into the effects of precipitation variability on groundwater storage, with implications for sustainable water management.[11], [12], [13], [14], [15].

2 Description of the study area

This study was conducted in the Saïss Plain (area $\approx 2200 \text{ km}^2$), which is located in north-central Morocco and

* Corresponding author: tsoulichaymae.rfm@gmail.com

includes 35 urban centers, among which 12 (Lqsir, Bittit, Sebaâ Ayouné, Ait Hrz lah, Ait Boubidmane, Dkhissa, Oued Jdida, Mhaya, Mejjate, Sidi Slimane Moul Lkifane, Ain Bida, and Oulad Tayeb) (Figure 1) are the ones with the most intensive agricultural activities owing to the presence of groundwater aquifers and fertile soils[16]. The soils of the Sais Plain (Fès–Meknès region) are generally brown calcareous soils with low organic matter content (<2%), sandy to loamy-sandy texture, and moderate clay enrichment in the deeper horizons. They exhibit a moderate water-holding capacity, high permeability, and a slightly to moderately alkaline pH (around 7.5–8.0), reflecting the calcareous and marly parent materials typical of the basin [17]. The main crops in the study area are vegetables and fruit trees[22,24]. Pesticides, especially glyphosate, is the most frequently used herbicides[21]. The groundwater of the Saïss plain plays a vital role in regional socio-economic development, providing drinking water for both local and neighboring centers and being an essential factor for agricultural activity development. In some rural regions, wells are the only source of drinking water[20,25].

2.1 Geological contexts

The main formations encountered in this aquifer are:

- Paleozoic: represented by a monotonous facies of fine quartzite schists intercalated with sandstone beds [24].
- Triassic: essentially made up of gypsiferous and saliferous clays (evaporitic deposits) with intercalations of doleritic basalts (700m thick) [25].
- Lias: the lias is formed essentially by massive and ruiniform limestone and dolomites. Miocene: the Miocene is formed mainly by sandstone limestone, gray marl (Messinian) and sandy marl ([26],[27]).
- Pliocene: The Pliocene is formed by sands with a carbonate matrix overmounting gray marls of the Messinian ([26]).
- Quaternary: it corresponds to a fluvial complex ([28]).
- Structurally, these carbonates are affected by several fractures causing a dislocation of different Liassic blocks and sometimes Pliocene-Quaternary limestone-travertine ([29]).

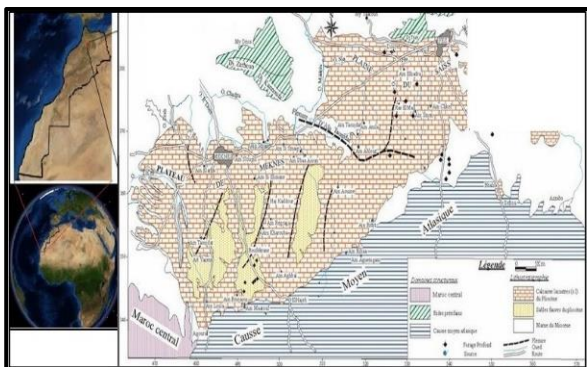


Fig. 1. Map of the geographical location of the study area and Geological ([30],[31]).

2.2 Hydrological and Hydrogeological contexts

In the Saïss system, there are two aquifer reservoirs:

- A free water table which develops at the level of the plain in Plio-Quaternary formations; The water table circulates mainly in sands, sandstones and locally in lacustrine limestones. This Plio-Quaternary surface water table has been recognized by a large number of boreholes, wells and springs (hydrogeological map at 1/1000000,[32] and [33]). Production flow rates: 1 to 20 l/s depending on the sector [34].
- With the transmissivities: $2 \cdot 10^{-5}$ to $1 \cdot 10^{-1} \text{ m}^2/\text{s}$. This strong variation of the transmissivity is due to the importance of the variation of the thickness and/or that of the permeabilities of the aquifer. And Permeability: $1 \cdot 10^{-5}$ to $5 \cdot 10^{-2} \text{ m/s}$. It is therefore a very heterogeneous environment, and flow direction from SSE to NNW [35].
- A deep aquifer that circulates mainly in the carbonate formations of the Lias. This aquifer is free at the level of the Causse and then sinks under the impermeable grounds of the Tertiary which put it in charge under the plain, the average water flux of all TMA aquifers is estimated at about 32-35 m^3/s , with 10 m^3/s transiting to the subterranean Saïss basin [29]. The flow rate of Bittit spring is from 1.3 to 1.5 m^3/s . The flow of Ribaa spring is from 0.02 to 0.32 m^3/s and that of Aguemguam spring is typical of a karst system, from 0 after a dry period to 0.53 m^3/s (Sebou-Fes Hydraulic Basin Agency 2008–2011) [36][37].

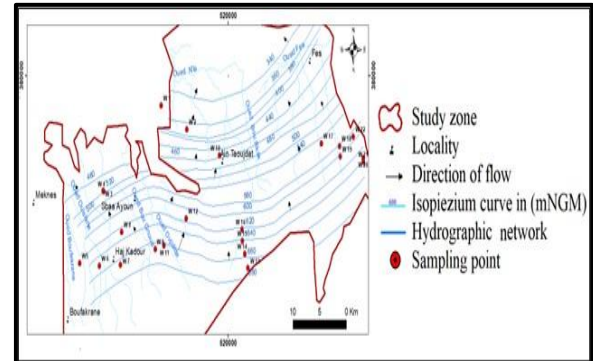


Fig. 2. The piezometric sketch map of the studied aquifer (March 2018).

The groundwater flows in this region are conditioned by two major fracture networks, mainly NE–SW and NW–SE directions [29];[37], and probably with a NW–SE preferential flow direction ([38]). A karstic complex water circulation is especially developed locally at the border of the two hydrogeological units[38].

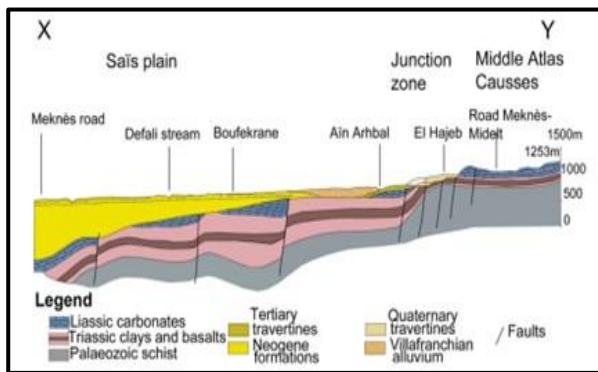


Fig.3. Geological section of the south Rifain groove according to the geological map of El Hajeb 1/1000000 Chamayou and al 1975).

The Saïss aquifer is generally characterized by mild winters with average rainfall of about 500–600 mm/year (Sebou-Fes Hydraulic Basin Agency, 2008–2011)[39][39]. This climate regime is also characterized by relatively constant temperature across the entire Saïss basin, which becomes slightly higher in the east [39]. During the past 50 years, the frequency of drought periods has increased ([40];[41]).

The Saïss plain is crossed by perennial Wadis: Wadi Boufekrane, Wadi Ouislane wadi Bou Gnoua, Wadi Oujdida, Wadi N'la, Wadi Boua Rakak and Wadi Fes (Figures 1 and 2) [42].

The Saïss system is characterized by an average superficial flow of around 5600 Mm³/year, which represents 29.4% of the global flow [43].

3 Materials and methods

3.1 Satellite data

Table 1 presents climate and TWS data are readily available and accessible for download from NASA and other websites, where monthly measurement files can be obtained. A Python application was developed to extract and visualize these datasets as maps or time series. In this study, GRACE and GRACE-FO TWS data were downloaded from the following URL in Table 1, in NetCDF format (CSR_GRACE_GRACE-FO_RL0602_Mascons_all-corrections.nc), covering the period from April 2002 to March 2024 (last updated: 2024-06-18). The data are plotted on a 1/4-degree longitudinal-lateral grid, but correspond to a 1x1-degree equal-area geodetic grid at the equator, which is the current native resolution for CSR RL06 mascon solutions. This new RL06 grid, with a resolution of 1/4 degree (compared to 1/2 degree in RL05), was designed to more accurately represent the coasts.

The final dataset includes monthly TWS anomalies in centimeters (cm) of equivalent water thickness from April 2002 to April 2020. Missing GRACE observations were interpolated linearly, using values from the two adjacent months.

Table1: source and availability of data.

Data source	Website
TWS GRACE and GRACE-FO data	https://www2.csr.utexas.edu/grace/RL0602_mascons.html
FLDAS Model Outputs	https://disc.gsfc.nasa.gov/datasets/FLDAS_NOAH01_C_GL_M_001/summary?keywords=FLDAS
IMERG data	https://gpm.nasa.gov/data/imerg
Soil moisture data	https://power.larc.nasa.gov/data-access-viewer/
Volume number	https://www2.csr.utexas.edu/grace/RL0602_mascons.html
Page number	https://disc.gsfc.nasa.gov/datasets/FLDAS_NOAH01_C_GL_M_001/summary?keywords=FLDAS
Year	https://gpm.nasa.gov/data/imerg
DOI	https://power.larc.nasa.gov/data-access-viewer/

3.2 The method of chronological decomposition of precipitation

There Decomposition method is an approach used in signal processing and image processing to decompose a signal or image into components that can be fine details or important structures.

A time series can be decomposed into three elements (Fig. 3).

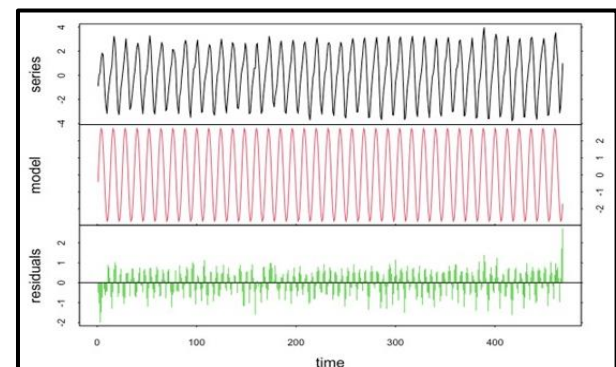


Fig. 4. Example of chronological decomposition of a precipitation series.

- The trend represents: The long-term evolution of the series studied; it reflects the “average” behavior of the (observed) series.
- The seasonal component or seasonality (seasonal) corresponds to a phenomenon that repeats itself at regular time intervals (periodic). In general, it is a seasonal phenomenon, hence the term seasonal variations.
- The residual component or noise or residue (random): These are irregular fluctuations of a random nature. They are obtained by removing trend and seasonal movements from the initial series. Additionally, the graphs in this study were taken from NASA data.

3.3 Man-Kendall Test

The Mann-Kendall (MK) statistic is a non-parametric test used for trend analysis. It was first introduced by Mann [44] and Kendall [45] derived the statistical distribution of the test [46]. This test is suitable for cases where the trend can be considered monotonic, and therefore no seasonal component is present in the data. One of the main advantages of the Mann-Kendall test is that: It is not a presupposition method in terms of data distribution, i.e., no assumptions are needed about the data distribution, as the prerequisite for this method is known as a non-parametric method[46].

3.4 Innovative trend test

The simple ITA methodology provides insight into trend analysis as it describes monotonic or non-monotonic upward or downward trends. In addition, it considers five trend conditions: monotonic and non-monotonic downward, monotonic and non-monotonic upward, and no trend [47].

The basic procedure of ITA is to divide the observation data from the first data values to the final data values into two equal parts and sort the two sub-data series in ascending order, respectively.

Based on two-dimensional Cartesian coordinates, the first half of the data value (Xi) is located on the horizontal axis (X-axis) and the second half of the data value (Xj) is located on the vertical axis (O-axis). The span of the two axes must be equal. The line (45°) divides the diagram into two similar triangles. If the data points accumulate on the 45° line, it is found that there is a trendless time series[48].

If all data points lie above (below) the 45° line in the upper (lower) region of the triangle, a monotonic upward (downward) trend is present in the time series data. Suppose the data points accumulate nonlinearly above (below) the 45° line in the upper (lower) region of the triangle. In this case, the time series data exhibits a non-monotonic upward (downward) trend.

The ITA method does not allow displaying the number of time series and subcategories. However, the new innovative trend analysis, as a new type of Şen methodology, indicates the mentioned trends and describes the number of data and subcategories.[47].

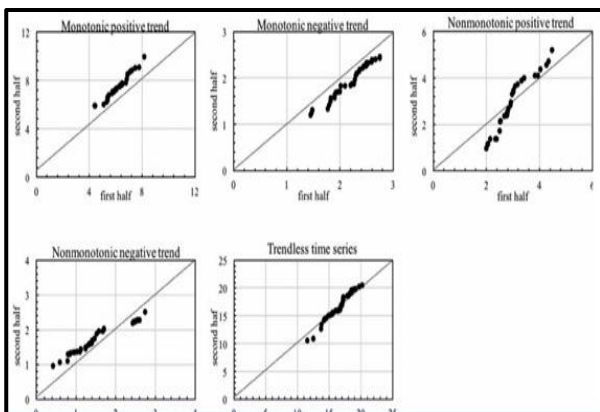


Fig. 5. Example of ITA innovative trend test.

3.5 Drought Index ISP

Table 2 shows the value of the drought indices as a function of the degree of humidity or dryness:

Droughts that impact water availability, agricultural production, and livestock activities are typically identified and characterized using drought indices. This study examines the potential of using the Standardized Precipitation Index (SPI) and the precipitation-based Standardized Precipitation-Evapotranspiration Index (SPEI) to replicate observed meteorological droughts in the Sais aquifer.

3.6 The TWS data analysis method

To calculate terrestrial water storage anomalies using the following equation[49]:

$$TWS = SW + SM + GWS + SWE \text{ (Eq. 1)}$$

With SW: Surface water

SM: Soil moisture

GWS: groundwater

SWE: Snow Water Equivalent

$$\text{Just like } GWS = TWS - SM \text{ (Eq. 2)}$$

4 Results and discussions

4.1 Climate context

Average precipitation data reveal clear seasonal patterns, with notable precipitation peaks during the winter months and significant decreases in the summer. January records the highest average precipitation, exceeding 60 mm, closely followed by December, November, February, and March, all of which display substantial precipitation levels (52-55 mm). These peaks correspond to the winter season, which generally brings the wettest months to semi-arid Mediterranean regions like Sais.

In contrast, the summer months (June to August) experience minimal rainfall, with August recording near-zero rainfall. This period is marked by the dry season, which exacerbates water shortages and reduces groundwater recharge. Transition months such as July and August experience a gradual decline in rainfall, reflecting the transition from winter to summer.

Analyzing historical rainfall trends (e.g., 12 mm in September, 2 mm in August, and moderate levels of 25 to 45 mm in May and April), the seasonal variability observed in this figure highlights the vulnerability of the Sais aquifer to drought and climate fluctuations. Prolonged periods of low rainfall, such as in summer, can put additional pressure on groundwater resources, requiring effective water management strategies to address recharge deficits during drought years ([50]).

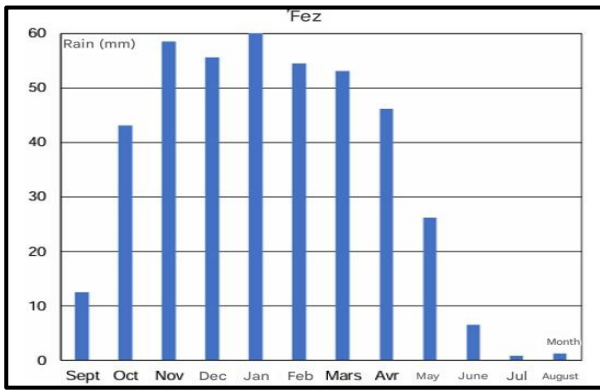


Fig. 6. Average monthly precipitation of the Sais aquifer

4.2 Chronological decomposition of precipitation in the Sais plain

The decomposition of the monthly precipitation time series shown in Figure 7 highlights the key components of rainfall variability over the observed period (2002-2020). The analysis separates the data into three main components: trend, seasonality and residuals.

(i) Original data (first part): The original rainfall series shows significant variability with multiple peaks and troughs over the years. Heavier rainfall events are visible between 2008 and 2011, and again around 2019 and 2020, indicating periods of increased rainfall intensity. The fluctuations highlight the erratic nature of rainfall in the study area.

(ii) Trend (second part): The trend component reveals long-term variations in precipitation. There was a notable decline in precipitation between 2002 and 2004, followed by a slight recovery and stabilization during the period 2004 to 2009. And from 2009 to 2015. From 2015 onwards, the trend shows another downward movement and a decrease in precipitation levels in recent years. This trend analysis reflects periods of drought and recovery, consistent with broader patterns of climate variability.

(iii) Seasonality (Part Three): The seasonal component highlights a consistent annual cycle of precipitation. Peaks occur during the winter months, reflecting the Mediterranean climate of the Sais region, where precipitation is concentrated in winter. This seasonal pattern remains consistent throughout the observed period, highlighting the regular presence of wet and dry seasons.

(iv) Residues (last part): Residuals represent irregular or random variations not captured by trend and seasonal components. These fluctuations are more pronounced in years with abnormally low precipitation, such as 2008 and 2018. They highlight events that deviate from typical patterns, likely caused by short-term climate factors or localized weather events.

In summary, time series decomposition effectively isolates the underlying components of precipitation variability. Seasonality is stable, driven by annual climate cycles, while the trend indicates periods of drought and recovery. The residuals show irregular fluctuations that can signal extreme weather events, highlighting the need for adaptive water resource management in response to climate variability.

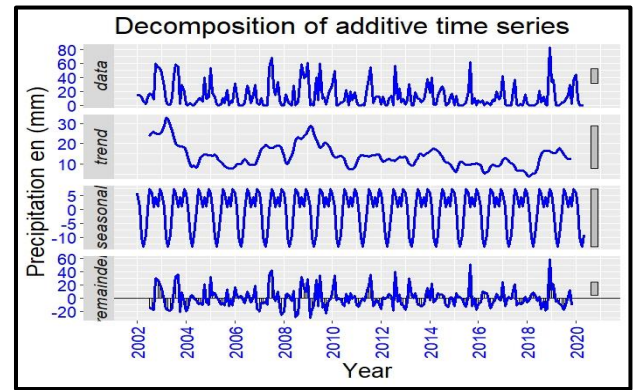


Fig. 7. Decomposition of precipitation data series (PM) in the Sais plain during the period 2002_2020

4.3 Innovative trend test to analyze temporal dynamics at the Sais aquifer

The results of the Mann-Kendall test on monthly precipitation trends at Sais station between 2002 and 2020 (Table 2) are presented in Table 2. The analysis reveals that there are no trends at the study area level. For example, January (p-value: 0.845) and February (p-value: 0.8533). Except in June the trend is significant with a downward direction.

However, the lack of significant trends in other months highlights the high variability and inconsistency of rainfall patterns over the years. This is consistent with the observed effects of drought and climate variability, which continue to impact groundwater resources in the Sais Basin, highlighting the vulnerability of the region's water table to climate change.

Table 2: Results of the Man-Kendall test at the Sais water table in 2002–2020

	P - value	Z	H0: No trend	Sen slope (cm / year)	Trend direction
January	0.228	- 1.2055	Yes	- 0.1515152	No trend
February	0.3843	- 0.86993	Yes	-0.1	No trend
March	0.633	1.3788	Yes	0.08695652	No trend
April	0.8365	- 0.20643	Yes	0	No trend
May	0.3228	- 0.98862	Yes	- 0.1470806	No trend
June	0.03641	- 2.0923	No	- 0.04347826	Drop
July	0.1011	- 1.6396	Yes	0	No trend
August	0.86	- 0.17635	Yes	0	No trend
September	0.7604	0.30498	Yes	0	No trend

October	0.9827	-0.021734	Yes	0	No trend
November	0.4874	-0.69441	Yes	-0.110043	No trend
December	0.2827	-1.0744	Yes	0	No trend
Annual	0.1653	1.3873	Yes	0.8225806	No tension

4.4 Trend test to analyze the temporal dynamics of precipitation in the Sais plain

The presented innovative trend methodology was applied to different precipitation time series recorded at the Sais gauging station. A mean precipitation time series was evaluated for the monthly time scale and a trend analysis was performed using the Innovative Trend Analysis (ITA) method. The results of the ITA approach were compared with those obtained by the Man-Kendall monotonic test applied to the original series. Each monthly value is represented by its estimated mean between the periods 2002 and 2020.

Figure 8 shows the results of the ITA method applied to the Sais station, reflecting monthly rainfall trends between 2002 and 2020. Each scatter plot corresponds to a specific month, where the x-axis represents rainfall values during the first half of the study period (2002-2011) and the y-axis represents values for the second half (2011-2020). The orange diagonal line serves as a 1:1 reference line, indicating no change in rainfall between the two periods. Points above this line signify an increasing trend, while points below this line indicate a decreasing trend in rainfall. The results highlight variable patterns across months, with notable increases in some months (e.g., November, December, and April), while others (e.g., July) show limited or no trends. These results provide a clear visualization of the temporal dynamics and monthly variability of precipitation in the Sais Plain during the study period.

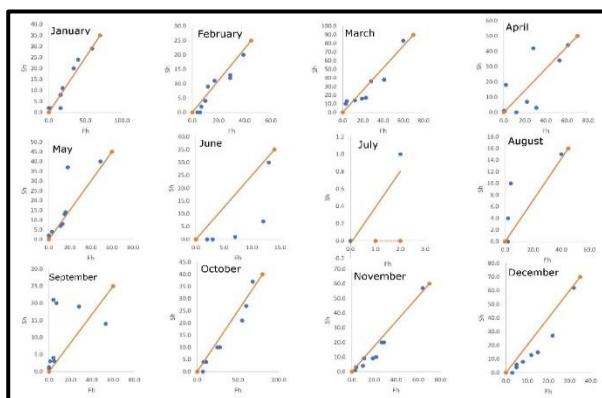


Fig. 8. Result of the ITA test on the aquifer

Innovative Trend Analysis (ITA) applied to monthly precipitation data at Sais station provides a detailed interpretation of precipitation trends by classifying the

data into three classes: low (< 20 mm), medium (20 to 40 mm) and high (> 40 mm). This classification facilitates the understanding of precipitation dynamics over the months. Interpretations are as follows:

- January: An increasing trend is observed for all categories (low, medium, high), indicating an increase in precipitation at all levels during the second half of the study period.
- February: A downward trend is observed for all precipitation categories, reflecting constant decreases.
- March: An upward trend at the low category level, and a downward trend for the other categories (Medium, Low), which indicates the climate is unstable at the level of the study area.
- April: An upward trend for the weak and strong categories, and a downward trend for the medium category.
- May: Precipitation shows an increasing trend in all categories, indicating an improvement in precipitation patterns for this month.
- June: Precipitation shows a decreasing trend for all categories, indicating a decrease in recharge.
- July: We find that there are not trends across all categories.
- August: We see increasing precipitation trends for all categories.
- September: For the low and medium categories, an upward trend is observed, indicating an increase in light and moderate precipitation. However, for the high category, a downward trend is observed, reflecting a decrease in heavy precipitation.
- October: An upward trend for the low category, suggesting a decrease in precipitation levels during this month. However, there is no significant trend at the high category level.
- November: The categories (low, medium) show a decreasing trend. However, the high category shows an increasing trend, which signifies the wet period at the Sais aquifer level.
- December: All categories (low, medium, high) show a downward trend, highlighting a decrease in precipitation.

This analysis highlights the seasonal variability of precipitation trends in the Sais Plain. The months of January, May, and August show consistent upward trends across all categories, indicating positive changes in precipitation. In contrast, February and January show clear downward trends across all categories. For June, July, August, September, and October, trends are minimal or nonexistent, reflecting stable or unchanged conditions. This information reveals a nuanced understanding of monthly precipitation dynamics and an overall downward trend in annual precipitation levels.

Figure 9 presents the results of the annual innovative trend analysis (ITA) test for the Sais Plain. In this figure, most of the blue points are located above the reference line, showing an increasing trend in annual precipitation over both periods. The significant clustering of points in the upper and middle range reflects an increase in precipitation intensity over time. The upward shift of the points relative to the reference line further confirms the overall positive trend. Only a few data points align with

or slightly below the line, showing rare cases of unstable or slightly decreasing precipitation. This result is consistent with more general findings regarding increasing trends in annual rainfall in the Sais Plain, which could have implications for water availability, agricultural productivity and resource management in the study area.

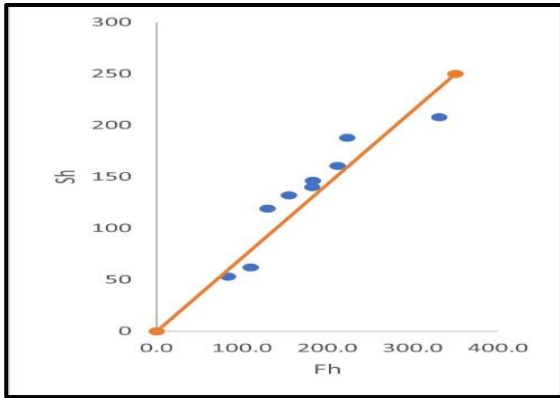


Fig. 9. Annual results of the ITA test at the Sais plain level

Based on the previous results of these tests, it is evident that the Innovative Trend Analysis (ITA) method offers greater reliability than the Mann-Kendall method. The Mann-Kendall analysis does not indicate any significant trend, while the ITA method reveals significant trends in different precipitation categories. For example, in January, it presents the increasing trend for all categories.

4.5 Analysis of satellite climate data

FLDAS Model

Figure 10 presents the decomposition of the Few Land Data Assimilation (FLDAS) precipitation time series into three components: trend, seasonality, and residual. The trend highlights three distinct periods of variation: an increasing trend from 2002 to 2008, a decreasing trend from 2008 to 2012, a stable increasing trend from 2012 to 2015, and a decreasing trend from 2015 to 2020. The seasonality component reveals a clear annual cycle, showing consistent periodic fluctuations in precipitation patterns over the years. The residual component (remainder) captures irregular variations that are not explained by trend or seasonality, with small deviations from the baseline, except for a notable increase in variability after 2016. Overall, the decomposition effectively distinguishes the underlying structure of the FLDAS precipitation data, which emphasize both long-term trends and recurring seasonal behavior in the Sais basin.

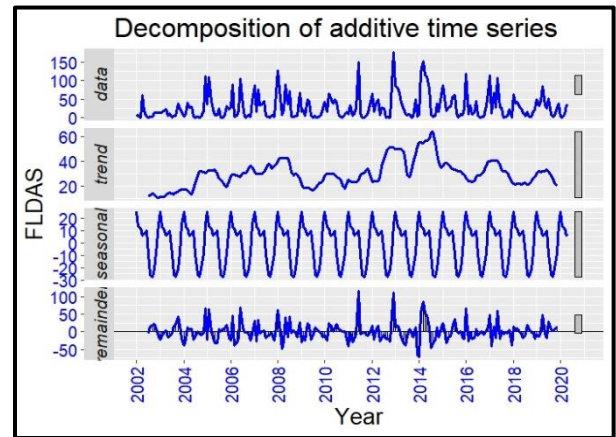


Fig. 10. Chronological decomposition of precipitation from the FLDAS model at the Sais plain level

IMERG model

Figure 11 shows the decomposition of the Integrated Multi-satellite Retrievals for GPM (IMERG) precipitation time series for the Sais water table into trend, seasonal, and residual components. The trend highlights three main phases: a decreasing trend from 2002 to 2008, an increasing trend from 2008 to 2012, and a subsequent decline from 2012 to 2020, consistent with the reported long-term variability. The seasonal component shows a clear pattern of alternating wet and dry seasons, indicating a consistent seasonal cycle of precipitation in the Sais region.

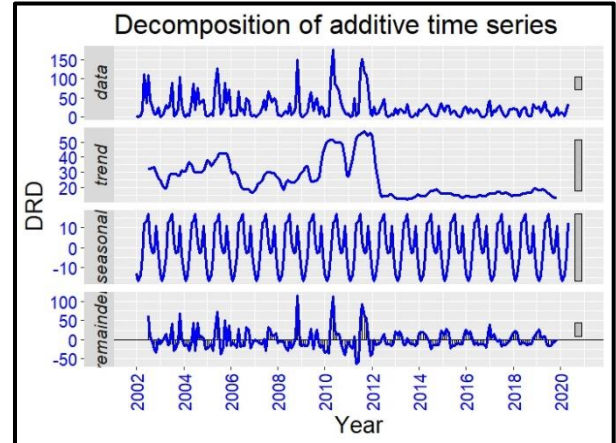


Fig. 11. Chronological decomposition of precipitation from the IMERG model at the Sais plain level

Finally, the residual component captures irregular fluctuations not explained by trend or seasonal patterns, with notable variability observed throughout the time series, particularly after 2008. This decomposition effectively captures annual cycles, long-term trends, and irregular variations in Integrated Multi-satellite Retrievals for GPM (IMERG) precipitation over the study period.

4.6 Precipitation correlation

Correlation of time series between models

Figure 12 illustrates the correlation between FLDAS, IMERG, and observed precipitation in the Sais aquifer.

IMERG, FLDAS, and measured precipitation data demonstrate a strong correlation, following similar trends over time, although IMERG data often show higher amplitudes, indicating a slight overestimation of precipitation. FLDAS data, on the other hand, remain relatively stable and show consistently lower values compared to other series. The overall pattern highlights that satellite-derived precipitation data (IMERG and FLDAS) capture the overall trend in measured precipitation, but IMERG data offer greater variability and better alignment with observed seasonal fluctuations. This comparison highlights the reliability of satellite products for monitoring precipitation trends while recognizing their tendency to overestimate precipitation levels compared to ground-based observations.

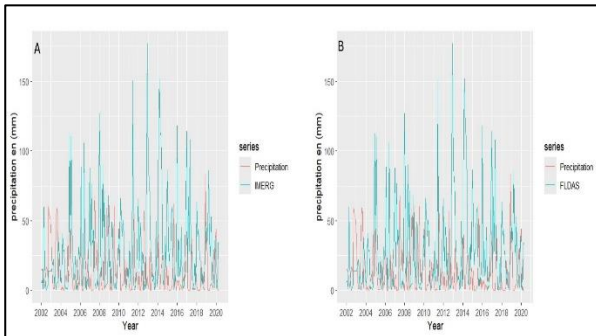


Fig. 12. (A) Correlation between the Precipitation and IMERG models; (B) Correlation between the Precipitation and FLDAS models at the Sais water table level.

4.7 Presentation of monthly average water storage anomalies derived from TWS_GRACE

The monthly mean TWS variations are sinusoidal with many peaks in spring and summer and a general decline in winter. It highlighted the effect of summer precipitation and flash floods. The GRCTellus Land RL06 version of the Gravity Recovery and Climate Experiment (GRACE) and Gravity Recovery and Climate Experiment (GRACE/FO) from these centers is available in two different solutions, namely spherical harmonic and mascon (mass concentration blocks). Figure 12 presents the TWS_GRACE-derived water storage anomalies for the Sais aquifer from 2002 to 2020. The trend highlights significant fluctuations in total water storage (TWS) anomalies over the years. Initially, from 2002 to 2011, water storage shows a gradual decrease with intermittent drops. Between 2011 and 2015, a notable peak phase occurs, indicating a period of higher water storage levels. However, after 2015, water storage anomalies show a steady downward trend, with significant reductions observed from 2017 onwards, reaching their lowest values in 2020. This trend suggests that after a period of relative stability and gain, the Sais aquifer has experienced sustained water loss, likely due to factors such as increased groundwater extraction, reduced recharge, or changing climatic conditions. The overall trajectory highlights a worrying decline in groundwater resources during the analyzed period.

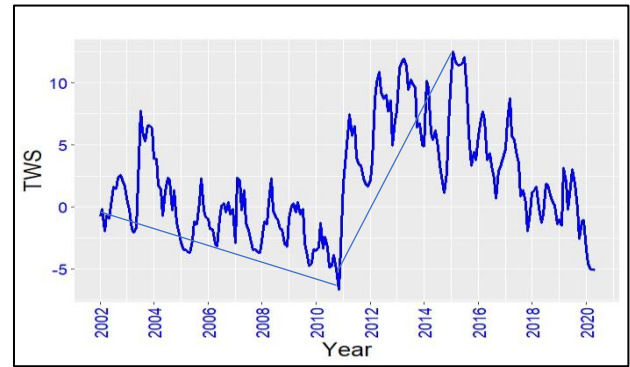


Fig. 13. Water storage anomalies derived from WS_GRACE in the Sais aquifer.

Table 3 presents the Mann-Kendall test results for TWS_GRACE over the three phases (2002-2020) in the Sais aquifer. The results reveal significant trends in terrestrial water storage (TWS) anomalies. In phase 1, the p-value is 0.07481, indicating a statistically significant increasing trend, with a Z MK value of 1.7816 and a Sen slope of -0.254 cm/year, reflecting a decrease in water storage. Phase 2, which shows the intermediate period, indicates a positive trend with a p-value of 0.2261, a Z MK value of 1.2105, and a Sen slope of 0.030 cm/year, showing a significant increase in water storage. However, in phase 3, the results highlight a pronounced decrease, with a p-value of 6.831×10^{-10} , a Z MK value of 6.17, and a steep Sen slope of -0.0155 cm/year, confirming a sharp decrease in TWS. These results highlight alternating phases of water gain and loss, with an overall decreasing trend in water storage, especially during the third phase, suggesting increasing pressure on groundwater resources in the Sais aquifer.

Table 3: Man-Kendall test for the three phases of TWS_GRACE

	The Mann-Kendall trend test				
	p-Value	H0: No trend	ZMK	Sen slope (cm/year)	Trend direction
Phase 1	0.07481	No	1.7816	-0.2538739	Increase
Phase 2	0.2261	Yes	1.2105	0.0301585	Increase
Phase 3	6.831×10^{-10}	No	-6.17	-0.01556101	Drop

4.8 Estimation of variations in groundwater storage at the Sais aquifer.

Figure 14 presents the calculation of groundwater storage (GWS) in the Sais plain using the relation $GWS = TWS - SM$ (Eq. 2), where SM represents soil moisture and TWS represents total terrestrial water storage.

Graph A (TWS): This graph shows the total terrestrial water storage anomalies from 2002 to 2020. The TWS exhibits significant fluctuations with a peak around

2006 to 2010, followed by a notable decline until 2020, reflecting a sustained reduction in total water storage.

Graph B (SM): This graph shows variations in soil moisture, which demonstrate a seasonal cycle with constant annual peaks and troughs throughout the study period. This indicates regular variability in soil moisture, likely due to precipitation and evapotranspiration.

Graph C (GWS): This graph plots groundwater storage as the difference between TWS and SM. GWS reveals a general declining trend, with notable reductions after 2016, indicating increasing groundwater depletion over time. The decline in GWS is more pronounced relative to fluctuations in soil moisture, highlighting the influence of groundwater extraction and reduced recharge rates.

In summary, while soil moisture (SM) remains relatively unstable across seasons, the decline in TWS and resulting trends in GWS highlight significant groundwater loss, particularly in recent years, indicating unsustainable water resource management in the Sais Plain.

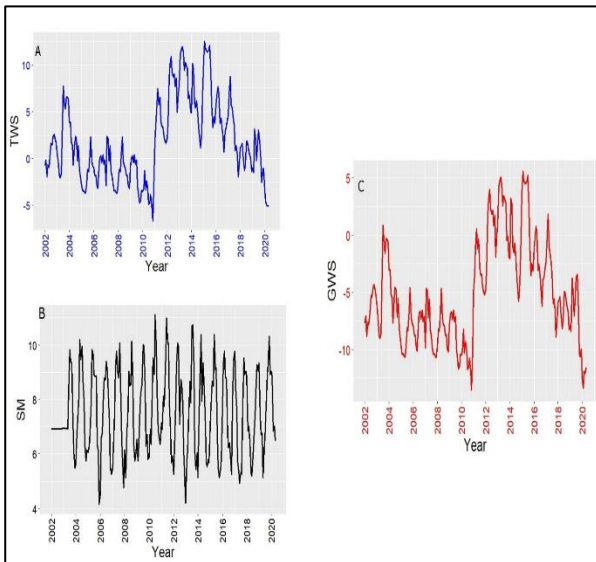


Fig. 14. Calculation of GWS from: (A) TWS; (B) SM; (C) GWS

The Mann-Kendall test results for the four-groundwater storage (GWS) phases in the Sais aquifer (Table 4) reveal significant trends over the study period.

In phase 1, the p-value is 0.0006757, indicating a statistically significant decreasing trend. The Z MK value of -3.3992 and a Sen slope of -0.029 cm/year reflect a notable decline in groundwater storage during this phase.

Phase 2 shows a negative trend, with a p-value of 0.2536, a Z MK value of -1.1416 and a Sen slope of -0.039 cm/year, indicating a sharp decrease in groundwater storage at the Sais aquifer level.

In phase 3, the p-value is 3.604e-09, which highlights a strong downward trend. The MK Z-value of -5.9014 and a steep Sen slope of -0.168 cm/year confirm a substantial decline in GWS, representing the most severe decline of all phases.

Table 4: Man-Kendall test for the three phases of the GWS at the Sais aquifer

	The Mann-Kendall trend test				
	ρ Value	H0: No trend	ZMK	Sen slope (cm/year)	Trend direction
Phase 1	0.0006757	No	-3.3992	-0.029161	Drop
Phase 2	0.2536	Yes	-1.1416	-0.039005	Drop
Phase 3	3.604e-09	No	-5.9014	-0.168570	Drop

In this study, the analysis reveals alternating periods of water gain and loss, with the final phase showing critical and accelerated depletion of groundwater resources in the Sais aquifer, suggesting increasing water stress and the need for improved groundwater management strategies.

4.9 Correlation between GWS and TWS

Figure 15 and Table 5 illustrate the relationship between terrestrial water storage (TWS) and groundwater storage (GWS) in the Sais aquifer from 2002 to 2020. The two series show a strong correlation, as trends and fluctuations closely align throughout the period. From 2002 to 2011, TWS and GWS show alternating increases and decreases, peaking around 2010–2015. After 2016, there is a consistent downward trend in TWS and GWS, with a particularly sharp decline observed after 2018, highlighting significant water loss. This decline reflects increasing groundwater depletion, likely due to increased extraction and reduced recharge. The strong agreement between the two series confirms that variations in TWS largely drive changes in GWS, highlighting the interdependence between terrestrial and groundwater storage within the Sais aquifer system.

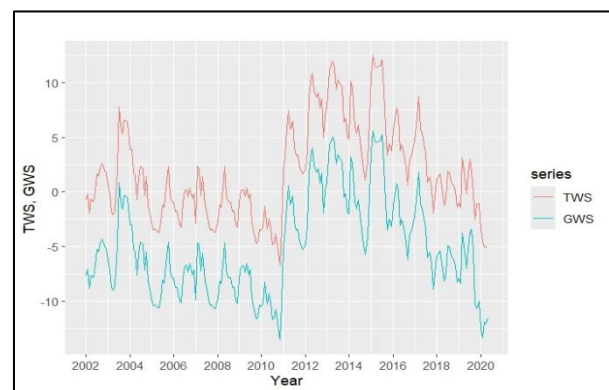


Fig. 15. Correlation between GWS and TWS of the Sais aquifer.

Table 5: Comparison between TWS and GWS at the Sais plain level

	The Mann-Kendall trend test		
	TWS	GWS	Trend direction
	Sen slope (cm·a ⁻¹)	Sen slope (cm·a ⁻¹)	
Phase 1	0.2538739	0.0006757	Drop
Phase 2	0.0301585	0.2536	High
Phase 3	-0.1556101	-0.1685704	Drop

4.10 Impact of drought on groundwater: - Relationship between precipitation and terrestrial water storage (TWS_GRACE)

Figure 16 highlights the relationship between precipitation (PM) and terrestrial water storage (TWS) anomalies over the period 2002-2020. The red graph represents TWS anomalies, while the green graph shows precipitation. A strong correlation is observed between the two parameters, indicating that precipitation variations significantly influence TWS trends. Precipitation peaks, particularly in 2002, 2004, and 2006, correspond to notable increases in TWS anomalies, demonstrating the direct impact of extreme precipitation events on terrestrial water storage. Conversely, drought periods such as 2011 and 2018 are marked by sharp decreases in TWS, reflecting reduced water availability due to insufficient precipitation. Over the long term, TWS anomalies show a gradual decline, suggesting the cumulative impact of droughts and reduced precipitation on terrestrial water storage. This analysis highlights the sensitivity of TWS to precipitation variability and highlights the important role of climate-related changes, such as droughts, in influencing water storage dynamics in the study area.

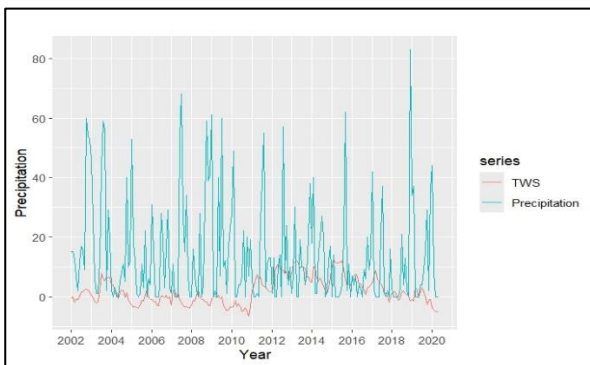


Fig. 16. Correlation between PM, TWS at the Sais water table level.

Effects of drought on water storage in the Sais aquifer Figure 17 illustrates the correlation between monthly precipitation (PM), terrestrial water storage (TWS) and groundwater storage (GWS) at the Sais water table during the study period (2002-2020). A clear negative trend in groundwater storage (GWS) is observed, reflecting a continuous decline in groundwater levels. TWS, represented by a linear trend, also shows a downward trajectory, indicating an overall loss of water mass in the catchment ([51]).

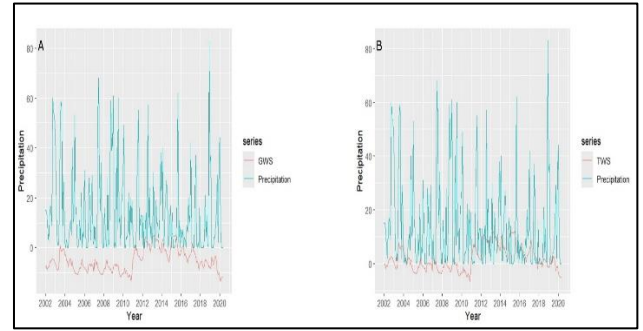


Fig. 17.(A) Correlation between PM and GWS; **(B)** Correlation between PM and TWS

This figure highlights a strong correlation between precipitation, TWS, and GWS, showing that fluctuations in precipitation have a direct impact on terrestrial and groundwater storage. In particular, periods of reduced precipitation correspond to sharp declines in TWS and GWS, confirming the adverse effects of climate variability and drought on the water balance. This analysis highlights the usefulness of GRACE satellite data for monitoring hydrological changes and supporting water resource management. While on-site observations remain essential, GRACE-derived data effectively validate observed trends in water volume loss, reinforcing the importance of integrating satellite data into environmental and water management strategies.

5 Conclusion

In conclusion, the analysis of rainfall intensity and water storage dynamics in the Sais Plain reveals significant temporal and spatial trends that highlight the region's vulnerability to climate variability and water scarcity. Scatter plot analysis indicates clear monthly variations in rainfall patterns, with some months showing consistently increasing trends, while others, such as June, July, August, September, and October, show a decline or no significant change. The Innovative Trend Analysis (ITA) method provides a more detailed and reliable insight into these trends, revealing that rainfall generally decreased during the study period, particularly during the second half of the analysis, with some months, such as January, February, and November, showing notable increases.

The decomposition of satellite-derived precipitation data (FLDAS and IMERG models) also supports the findings, highlighting the cyclical nature of precipitation and climate-induced variability. Analysis of terrestrial water storage (TWS) and groundwater storage (GWS) also highlights a worrying decline in water resources, with the Sais aquifer showing significant water loss, particularly after 2013. The correlation between precipitation, TWS, and GWS indicates a strong correlation, with reduced precipitation directly leading to lower water storage levels. Furthermore, the impact of drought on groundwater resources is evident, as periods of reduced precipitation align with sharp declines in water storage and increased water stress.

These results highlight the urgent need to improve water resource management and strategic planning, particularly in the face of increasing climate variability and frequent droughts. Integrating satellite data, such as GRACE and piezometric level analysis, provides a valuable tool for monitoring hydrological changes and supporting sustainable water management in the Sais aquifer. Ultimately, addressing the challenges posed by declining water availability will require a combination of effective resource management strategies, climate change adaptation measures, and careful monitoring of trends in terrestrial and groundwater storage.

6 References

- [1] H. Ouakhir et al., « CHANGES IN RIVER BANK MORPHOLOGY IN A SMALL MEANDER OF EL ABID RIVER, ATLAS MOUNTAINS, MOROCCO », *AgricultForest*, vol. 69, no 3, sept. 2023, doi: 10.17707/AgricultForest.69.3.14.
- [2] A. Salhi et al., « Rainfall distribution and trends of the daily precipitation concentration index in northern Morocco: a need for an adaptive environmental policy », *Applied Sciences*, vol. 1, p. 277, mars 2019, doi: 10.1007/s42452-019-0290-1.
- [3] N. Ennaji, O. Hasan, M. Abahrour, V. Spalevic, et B. Dudic, « Impact of watershed management practices on vegetation, land use changes, and soil erosion in River Basins of the Atlas, Morocco », *Notulae Botanicae Horti Agrobotanici Cluj-Napoca*, vol. 52, p. 1-12, mars 2024, doi: 10.15835/nbha52113567.
- [4] N. Ennaji, H. Ouakhir, S. Halouan, et M. Abahrour, « Assessment of soil erosion rate using the EPM model: case of Ouaoumana basin, Middle Atlas, Morocco. », *IOP Conf. Ser.: Earth Environ. Sci.*, vol. 1090, no 1, p. 012004, oct. 2022, doi: 10.1088/1755-1315/1090/1/012004.
- [5] F. Wang et al., « Re-evaluation of the Power of the Mann-Kendall Test for Detecting Monotonic Trends in Hydrometeorological Time Series », *Front. Earth Sci.*, vol. 8, févr. 2020, doi: 10.3389/feart.2020.00014.
- [6] « Geochemical Study of the Angads Groundwater (North-East Morocco) | 5 | ». Consulté le: 15 mars 2025. [En ligne]. Disponible sur: <https://www.taylorfrancis.com/chapters/edit/10.1201/9781003436218-5/geochemical-study-angads-groundwater-north-east-morocco-latifa-taoufiq-iliyas-kacimi-mohamed-saadi-jamal-mabrouki-nordine-nouayti-nadia-kassou-tarik-bouramtane-karima-el-mouhdi>
- [7] « Taoufiq, L., I. Kacimi, M. Saadi, N. Nouayti, N.... - Google Scholar ». Consulté le: 15 mars 2025. [En ligne]. Disponible sur: https://scholar.google.com/scholar?hl=fr&as_sdt=0%2C5&q=Taoufiq%2C+L.%2C+I.+Kacimi%2C+M.+Saadi%2C+N.+Nouayti%2C+N.+Kassou+a nd+K.+El-Mouhdi+%282024%29.+%22Monitoring+the+Overall+Quality+of+Groundwater+Using+a+Geographic+Information+System+in+the+Angads+Plain+%28Oujda%2C+Morocco%29.%22+The+Scientific+World+Journal+2024%281%29%3A+7511804.&btnG=
- [8] Y. S. Güçlü, « Multiple Şen-innovative trend analyses and partial Mann-Kendall test », *Journal of Hydrology*, vol. 566, p. 685-704, nov. 2018, doi: 10.1016/j.jhydrol.2018.09.034.
- [9] « First Report of *Halopithys incurva* (Rhodomelaceae, Rhodophyta) from the Marchica Lagoon of Nador (North-Est Morocco, Mediterranean) | E3S Web of Conferences ». Consulté le: 15 mars 2025. [En ligne]. Disponible sur: https://www.e3s-conferences.org/articles/e3sconf/abs/2024/57/e3sconf_joe4_01002/e3sconf_joe4_01002.html
- [10] E. M. Azzirgue et al., « Interactions evaluation between the Jouamaa Hakama groundwater and Ouljat Echatt river in the north of Morocco, Using hydrochemical modeling, multivariate statistics and GIS », *Water*, vol. 15, no 9, p. 1752, 2023.
- [11] N. Abou Zaki, A. Torabi Haghighi, P. M. Rossi, M. J. Tourian, et B. Kløve, « Monitoring Groundwater Storage Depletion Using Gravity Recovery and Climate Experiment (GRACE) Data in Bakhtegan Catchment, Iran », *Water*, vol. 11, no 7, p. 1456, juill. 2019, doi: 10.3390/w11071456.
- [12] H. Chen, W. Zhang, N. Nie, et Y. Guo, « Long-term groundwater storage variations estimated in the Songhua River Basin by using GRACE products, land surface models, and in-situ observations », *Science of the total environment*, vol. 649, p. 372-387, 2019.
- [13] Y. Cheng et al., *GRACE: Loss-Resilient Real-Time Video Communication Using Data-Scalable Autoencoder*. 2022.
- [14] M. Hamdi, « Réponse d'un système aquifère aux changements climatiques et au stress anthropique : apport de la modélisation numérique et la gravimétrie satellitaire », 2023. doi: 10.13140/RG.2.2.25391.51361.
- [15] N. A. A. Mukhtar, A. H. M. Din, N. A. Zulkifli, M. H. Hamden, A. H. Omar, et A. I. A. Hamid, « EVALUATION OF GROUNDWATER STORAGE CHANGES USING SATELLITE GRAVIMETRY MISSION IN PENINSULAR MALAYSIA », *Int. Arch. Photogramm. Remote Sens. Spatial Inf. Sci.*, vol. XLVIII-4/W6-2022, p. 253-259, févr. 2023, doi: 10.5194/isprs-archives-XLVIII-4-W6-2022-253-2023.
- [16] M. Berriane, 2002, « Le maillon intérieur : la région de Fès-Meknès, in Maroc : régions, pays, territoires, JF Troin(édit.), Maisonneuve et Larose, Paris, Tariq, Rabat, pp. 133-151 ».
- [17] D. Touhtouh, E. M. Faleh, et R. el halimi, « Physical and chemical characterization of three types of soils of Saïs, Morocco », vol. 6, p. 3582-3593, janv. 2015.
- [18] I. Berni, B. Imane, E. R. Karima, N. Chakib, A. Mariam, et Z. Ahmed, « Pesticide Use Pattern

- among Farmers in a Rural District of Meknes: Morocco », *Open Access Library Journal*, vol. 3, no 12, p. 720-726, déc. 2016, doi: 10.4236/oalib.1103125.
- [19] M. Baccar, A. Bouaziz, P. Dugué, et P.-Y. L. Gal, « Shared environment, diversity of pathways: dynamics of family farming in the Saïss Plain (Morocco) », *Reg. Environ. Change*, vol. 17, p. 739-751, 2017, doi: 10.1007/s10113-016-1066-4.
- [20] I. Berni et al., « Understanding farmers' safety behavior regarding pesticide use in Morocco », *Sustainable Production and Consumption*, vol. 25, p. 471-483, janv. 2021, doi: 10.1016/j.spc.2020.11.019.
- [21] I. Berni et al., « Understanding farmers' safety behavior regarding pesticide use in Morocco », *Sustainable Production and Consumption*, nov. 2020, doi: 10.1016/j.spc.2020.11.019.
- [22] R. Fofack, M. Kuper, et O. Petit, « Hybridation des règles d'accès à l'eau souterraine dans le Saïss (Maroc) : entre anarchie et Léviathan ? », *Études rurales*, no 196, Art. no 196, sept. 2015, doi: 10.4000/etudesrurales.10427.
- [23] I. Berni, A. Menouni, E. G. Ibrahim, L. Godderis, R.-C. Duca, et E. Samir, « Health and ecological risk assessment based on pesticide monitoring in Saïss plain (Morocco) groundwater », *Environmental Pollution*, vol. 276, févr. 2021, doi: 10.1016/j.envpol.2021.116638.
- [24] L. Taoufiq et al., « Assessment of Physicochemical and Bacteriological Parameters in the Angads Aquifer (Northeast Morocco): Application of Principal Component Analysis and Piper and Schoeller-Berkaloff Diagrams », *Applied and Environmental Soil Science*, vol. 2023, p. 1-14, janv. 2023, doi: 10.1155/2023/2806854.
- [25] L. Taoufiq et al., « Determination of the Physico-Chemical and Bacteriological Characteristics of the Groundwater of Angads (Oujda, Morocco) by Principal Component Analysis (PCA) », in *Technical and Technological Solutions Towards a Sustainable Society and Circular Economy*, J. Mabrouki et A. Mourade, Éd., in *World Sustainability Series.*, Cham: Springer Nature Switzerland, 2024, p. 509-518. doi: 10.1007/978-3-031-56292-1_41.
- [26] L. Ait Brahim et al., « Paleostress evolution in the Moroccan African margin from Triassic to Present », *Tectonophysics*, vol. 357, no 1, p. 187-205, nov. 2002, doi: 10.1016/S0040-1951(02)00368-2.
- [27] « Management of inverted papilloma - Myers - 1990 - The Laryngoscope - Wiley Online Library ». Consulté le: 14 mars 2025. [En ligne]. Disponible sur: <https://onlinelibrary.wiley.com/doi/abs/10.1288/0005537-199005000-00008>
- [28] M. Ahmamou, « Etude sédimentologique des calcaires lacustres (ploiquaternaire) du bassin de Fès-Meknès (Maroc) », PhD Thesis, Thèse de 3 cycle, Univer. Aixmarseille III, 1987.
- [29] A. Boutsougame et al., « Impact of geology and climate change on wetlands: Case of Lake Aguelmam Azegza (Middle Atlas, Morocco) », *E3S Web Conf.*, vol. 337, p. 01007, 2022, doi: 10.1051/e3sconf/202233701007.
- [30] J. MARGAT et P. TALTASSE, « EVOLUTION MORPHOLOGIQUE ET TECTONIQUE RECENTE DANS LE BASSIN LACUSTRE DE FES-MEKNES (MAROC) », *COMPTES RENDUS HEBDOMADAIRES DES SEANCES DE L ACADEMIE DES SCIENCES*, vol. 237, no 22, p. 1424-1426, 1953.
- [31] A. Rhazi, A. Essahlaoui, A. Hmaid, et A. Ouali, « Etude De La Vulnerabilite Aux Risques D'inondations Dans La Ville De Meknes. Apport Des Sig, Du Mnt Et Des Modeles Empiriques », *Eur Sci J ESJ*, vol. 13, no 36, p. 102, 2017.
- [32] J. Margat, « SUR LA TERMINOLOGIE DES CARTES DES EAUX SOUTERRAINES: Essais de Definition », *International Association of Scientific Hydrology. Bulletin*, vol. 5, no 2, p. 53-55, juin 1960, doi: 10.1080/02626666009493171.
- [33] H. SAHBI, A. ESSAHLAOU, A. EL OUALI, et N. EL YAMINE, « Etude hydrogéologique de la formation aquifère superficielle du plateau de Meknès (Maroc) à partir des données géoélectriques. 15 », in *Colloque des bassins sédimentaires marocains*, Oujda, 1999, p. 27-29.
- [34] L. Taoufiq et al., « Assessment of the Piezometric and Rainfall Levels of the Groundwater in the Angads Plain, Northern Morocco. », *Tropical Journal of Natural Product Research*, vol. 7, no 12, 2023, Consulté le: 15 mars 2025. [En ligne]. Disponible sur: https://www.researchgate.net/profile/Ilham-Lhilali/publication/379182619_Tropical_Journal_of_Natural_Product_Research_Original_Research_Article_Assessment_of_the_Piezometric_and_Rainfall_Levels_of_the_Groundwater_in_the_Angads_Plain_Northern_Morocco/links/65fe1ce3a8ba573a1cf050f/Tropical-Journal-of-Natural-Product-Research-Original-Research-Article-Assessment-of-the-Piezometric-and-Rainfall-Levels-of-the-Groundwater-in-the-Angads-Plain-Northern-Morocco.pdf
- [35] O. Saadi, F. Dimane, N. Nouayti, A. Nouayti, et A. Bourjila, « Study of Hydrochemical Characteristics in the Middle Moulouya Basin of Morocco », *Ecological Engineering & Environmental Technology*, vol. 25, 2024, Consulté le: 15 mars 2025. [En ligne]. Disponible sur: <https://yadda.icm.edu.pl/baztech/element/bwmeta1.element.baztech-a612431b-2900-4641-8322-fc840585c7bb>
- [36] N. Nouayti, D. Khattach, et M. Hilali, « Evaluation de la qualité physico-chimique des eaux souterraines des nappes du Jurassique du haut bassin de Ziz (Haut Atlas central, Maroc)[Assessment of physico-chemical quality of groundwater of the Jurassic aquifers in high

- basin of Ziz (Central High Atlas, Morocco)] », *Journal of Materials and Environmental Science*, vol. 6, no 4, p. 1068-1081, 2015.
- [37] « Controls on Ground Water Chemistry in the Central Couloir Sud Rifain, Morocco - Benaabidate - 2010 - Groundwater - Wiley Online Library ». Consulté le: 14 mars 2025. [En ligne]. Disponible sur: <https://ngwa.onlinelibrary.wiley.com/doi/abs/10.1111/j.1745-6584.2008.00533.x>
- [38] K. Qarqori, « Contribution à l'étude du Réservoir Discontinu et Karstique des Causses Moyen-Atlasiques et de sa Jonction Avec le Bassin de Saïs par Télédétection Spatiale et Imagerie Géophysique [Contribution to the study of the discontinuous and karstic reservoir of the Middle Atlasic Causses and its junction with the Saïs Basin by Remote Sensing and Geophysical Imagery] », Thèse Doctorat, Univ. My Ismaïl. 183p, 2015.
- [39] N. Nouayti et al., « Determination of physicochemical water quality of the ghis-nekor aquifer (Al hoceima, Morocco) using hydrochemistry, multiple isotopic tracers, and the geographical information system (GIS) », *Water*, vol. 14, no 4, p. 606, 2022.
- [40] « Long-term drought severity variations in Morocco - Esper - 2007 - Geophysical Research Letters - Wiley Online Library ». Consulté le: 14 mars 2025. [En ligne]. Disponible sur: <https://agupubs.onlinelibrary.wiley.com/doi/full/10.1029/2007GL030844>
- [41] B. Damnati et al., « Recent environmental changes and human impact since mid-20th century in Mediterranean lakes: Ifrah, Iffer and Afourgagh, Middle Atlas Morocco », *Quaternary International*, vol. 262, p. 44-55, juin 2012, doi: 10.1016/j.quaint.2011.09.028.
- [42] M. Najy, F. Z. Talbi, H. Ech-chafay, O. Akkaoui, N. Nouayti, et D. Belghyti, « Characteristics and Assessment of Heavy Metals in the Water of Lake Sidi Boughaba (Kenitra, Morocco) », in *Innovations in Smart Cities Applications Volume 5*, vol. 393, M. Ben Ahmed, A. A. Boudhir, İ. R. Karaş, V. Jain, et S. Mellouli, Éd., in *Lecture Notes in Networks and Systems*, vol. 393, Cham: Springer International Publishing, 2022, p. 621-628. doi: 10.1007/978-3-030-94191-8_50.
- [43] M. Najy et al., « Ecological risk assessment of heavy metals in the Sidi Boughaba Lake, Morocco », *Journal of Water and Land Development*, 2023, Consulté le: 15 mars 2025. [En ligne]. Disponible sur: <https://yadda.icm.edu.pl/baztech/element/bwmeta1.element.baztech-7422f9d7-a169-481b-8dbb-537d5d2cf923>
- [44] H. B. Mann, « Nonparametric Tests Against Trend », *Econometrica*, vol. 13, no 3, p. 245-259, 1945, doi: 10.2307/1907187.
- [45] K. Kendall, « Thin-film peeling-the elastic term », *J. Phys. D: Appl. Phys.*, vol. 8, no 13, p. 1449, sept. 1975, doi: 10.1088/0022-3727/8/13/005.
- [46] A. Drouiche, F. Nezzal, et M. Djema, « Variabilité interannuelle des précipitations dans la plaine de la Mitidja en Algérie du Nord », *rseau*, vol. 32, no 2, p. 165-177, oct. 2019, doi: 10.7202/1065205ar.
- [47] Y. Alifujiang, J. Abuduwaili, et A. Abliz, « Precipitation trend identification with a modified innovative trend analysis technique over Lake Issyk-Kul, Kyrgyzstan », *Journal of Water and Climate Change*, vol. 14, no 6, p. 1798-1815, juin 2023, doi: 10.2166/wcc.2023.413.
- [48] T. Ahalli et al., « Impact of precipitation intensity and drought patterns on groundwater storage fluctuations within the Ghis-Nekor aquifer (Morocco) », *Ecological Engineering & Environmental Technology*, vol. 26, no 2, p. 323-341.
- [49] C. Pascal, « Cartographie multi-échelle des ressources en eau sur les régions irriguées: une approche par télédétection multi-capteurs », PhD Thesis, Université Paul Sabatier-Toulouse III, 2022. Consulté le: 11 juillet 2024. [En ligne]. Disponible sur: <https://theses.hal.science/tel-04139330/>
- [50] O. Hasan et M. E. Ghachi, « Temporal Dynamic of Soil Erosion and Rainfall Erosivity Within Srou River Basin (Middle Atlas / Morocco) », *Am. J. Mech. Appl.*, vol. 11, no 1, Art. no 1, mai 2023, doi: 10.11648/j.ajma.20231101.11.
- [51] C. Meng, D. Tian, H. Zeng, Z. Li, C. Yi, et S. Niu, « Global soil acidification impacts on belowground processes », *Environ. Res. Lett.*, vol. 14, no 7, p. 074003, juill. 2019, doi: 10.1088/1748-9326/ab239c.